

Al/Cu Laminated Wire Conductors; Effect of Stacking Sequence on Residual Stress

KUNČICKÁ, L.^{1,2a}, KOCICH, R.^{2,b}

¹Institute of Physics of Materials, Academy of Science of Czech Republic, Brno, 61662, Czech Republic

²Faculty of Materials Science and Technology, VŠB-Technical University of Ostrava, 70833 Ostrava 8, Czech Republic

^akuncicka@ipm.cz, ^bradim.kocich@vsb.cz

Keywords: rotary swaging, clad composite, residual stress, microstructure

Abstract. The presented study deals with preparation of Al-Cu clad composite wires with two different stacking sequences via the intensive plastic deformation technology of rotary swaging (RS). The aim of the work was to provide detailed characterization of the effects of RS on the development of structure and residual stress within the composites and their components. The results showed that fine more or less equiaxed grains with no prevailing preferential orientations were present within all the Al and Cu composites' components of the final 5 mm thick wires, which points to the occurrence of dynamic recovery/recrystallization during processing. The analyses of grains misorientations revealed that residual stress was locally present primarily in the Cu components; the Al components did not exhibit substantial presence of residual stress, which is in accordance with the observed structure relaxation. The tensile tests of the swaged composites revealed both the stacking sequences to exhibit comparable ultimate tensile strength, however, the plasticity differed notably.

Introduction

Research and development in virtually all the industrial fields has led to the emergence of numerous modern components, as well as to the introduction of a variety of innovative materials, such as plasma and laser melted alloys [1], (pseudo)alloys manufactured via powder metallurgy [2], high entropy alloys (HEAs) or multi-principal element (MPE) alloys [3,4], hierarchical and hybrid materials [5,6], functionally graded materials [7], and composites [8]. The latter can be of various types; the most characteristic are the Metal Matrix Composites (MMCs) [9] offering the advantages of the individual component metals and, at the same time, benefiting from the additions of dispersed particles/fibres. Nevertheless, laminated and clad composites consisting of several layers of various metals, each one of which introduces characteristic properties to create their unique combination within the final product, are also popular, since composites combining several metals together feature enhanced combinations of properties when compared to the individual components [10–13].

Among the widely researched composite systems consisting of bulk metallic components, i.e. layers, is the Al/Cu one [14]. Copper is favoured for its excellent electric and heat conductivity, while aluminium is preferred for its high conductivities and favourable combination of low density and reasonable strength [15]. Beside these (and other) advantages, both the metals have a wide applicability, e.g. in the automotive and electrotechnics. However, they both feature the tendency to form intermetallic compounds when in contact, i.e. to form intermetallics at mutual interfaces, especially at high (elevated) temperatures.

Clad composites consisting of multiple layers bond together at mutual interfaces are typically produced by welding, however, welding can introduce local structure modifications and formation of brittle intermetallics [16]. Nevertheless, clad composites can also be fabricated at room temperature via methods of (intensive) plastic deformation, which provides an advantageous solution for production of clad composites at room temperatures, or under cold conditions. Considering the layered Cu/Al composites, even post-process heat treatment at temperatures above 300°C has been documented to introduce the development of intermetallics, which makes post-processing of these composites unfavourable despite the fact that it also supports structure restoration and grain refinement within both the metals [17]. Methods of severe plastic deformation (SPD) are especially advantageous for preparation of clad composites since they can typically be performed at low/room temperatures. Among the widely researched and/or used SPD methods are, e.g., equal channel angular pressing (ECAP) [18,19] and its modifications (ECAP-PBP [20], TCAP [21], TCMAP [22], etc.), high pressure torsion (HPT) [23], accumulative roll bonding (ARB) [24], and rotary swaging (RS) [25–27], which was used to manufacture the herein studied composites.

Rotary swaging (RS) is a versatile industrially applicable intensive plastic deformation technology enabling to manufacture various axially symmetrical products via a repeated action of a set of rotating dies, which incrementally affects the surface of the work-piece with compressive radial forces and thus introduces a favourable combination of shear and compressive strains [28]. The nature of the process enables to avoid large stress gradients and supports progressive grain refinement, which introduces improvement of mechanical and utility properties [29].

The presented study deals with preparation of Al-Cu clad composite wires with two different stacking sequences via room temperature rotary swaging. The aim of the work was to provide a detailed characterization of the effects of RS on the development of structure and residual stress within the 5 mm swaged composite wires.

Experimental

The originally used metals were commercially pure (CP) copper (with 0.002 wt.% O, 0.015 wt.% P, and 0.002 wt.% Zn), and CP electro-conductive aluminium (with 0.20 wt.% Si, 0.25 wt.% Fe, and 0.05 wt.% Cu). The clad composites fabricated from the Cu and Al were gradually swaged from the original 30 mm diameter to the final wires having 5 mm in diameter. Both the stacking sequences originally consisted of a sheath with 30 mm in diameter, and 19 reinforcing wires having 3 mm in diameter each. The *stacking sequence I* consisted of Al sheath and Cu wires, whereas the *stacking sequence II* consisted of Cu sheath and Al wires. To acquire the idea of the composite design, Fig. 1 depicts a cross-sectional cut through the *stacking sequence I* swaged composite with 10 mm in diameter.

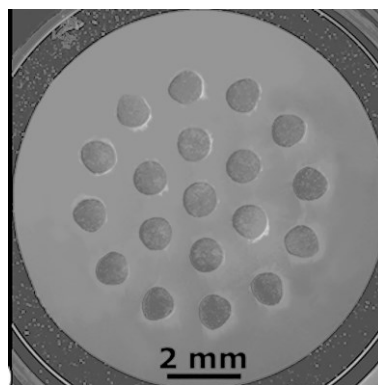


Fig. 1: Example of cross-sectional cut through investigated composites (sheath and 19 wires)

Detailed structure analyses of the swaged wires were performed by scanning electron microscopy (SEM); Tescan Lyra 3 FIB/SEM microscope equipped with a NordlysNano detector for electron back-scattered diffraction (EBSD) analyses was used. The scanned images were evaluated with the help of OXFORD Instruments [30] and LEM3 Laboratories [31] software. Microhardness measurements were performed using Zwick/Roell equipment; the average HV values for the Al/Cu sheath were calculated from a set of ten individual values measured across the particular composite cross-sectional cut (excluding the wires), while the average HV values for the wires were calculated from a set of ten individual values measured throughout all the wires. The samples for all the analyses were prepared via manual grinding on SiC papers and final diamond suspension polishing. For EBSD analyses, the samples were eventually polished electrolytically.

Results and Discussion

Mechanical properties. The original values of microhardness for the Cu and Al composite components were 84.5 HV, and 25.7 HV, respectively. The results of HV measurements of the 5 mm room-temperature swaged composites of *stacking sequence I* showed that the average HV value of the Al sheath was 55.1 HV, while for the Cu wires it was 106.9 HV. The HV measurements of the 5 mm room-temperature swaged composites of *stacking sequence II* then resulted in the average HV value of the Cu sheath to be 108.3 HV, while for the Al wires it was 34.4 HV.

Whereas the HV values of the Cu components were comparable for both the stacking sequences, the average HV values of the Al component differed significantly. This phenomenon can be explained by the mutual effect of the following two factors: 1) the RS process affects primarily the peripheral regions of the swaged piece, by the effect of which the imposed strain was primarily “consumed” by the prevailing volume of the Al sheath for *stacking sequence I* [32]; and 2) the maximum work hardening ability of the Al sheath was achieved during swaging (given by the intrinsic properties of Al, especially the stacking fault energy) [15].

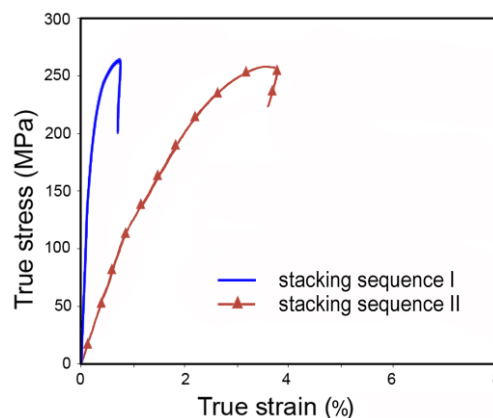


Fig. 2: Tensile stress-strain curves for both 5 mm swaged composite wires

The stress-strain curves resulting from the tensile tests of both the 5 mm swaged composite wires are depicted in Fig. 2. The tensile tests of the swaged composites revealed both the stacking sequences to exhibit comparable ultimate tensile strengths, however, the plasticity differed notably. Whereas *stacking sequence II* composite exhibited the elongation to failure of ~3.5%, composite with *stacking sequence I* exhibited the plasticity of less than 1%. The stress-strain curve for *stacking sequence I* featured a steep increase at quite small deformations, i.e. *stacking sequence I* exhibited rapid work hardening at the expense of

plasticity. The 5 mm *stacking sequence II* also exhibited rapid work hardening. Nevertheless, its intensity was not as high as for *stacking sequence I* (the slope of the stress-strain curve was less steep).

The relatively high strength of the swaged composites can primarily be attributed to the high volume fraction of Cu for *stacking sequence II*, and to the maximum achieved work hardening of the Al sheath for *stacking sequence I* (this supposition corresponds to the increased microhardness, as mentioned above). On the other hand, the imposed shear strain supports increase in plasticity for the Cu [33]. This factor was most probably the reason for the increased plasticity of *stacking sequence II*, whereas the plasticity of *stacking sequence I* was exhausted given by the major portion of work-hardened Al.

Structure analyses. The structure observations revealed the presence of fine more of less equiaxed grains within all the Al and Cu composites' components; the examples document Figs. 3a and 3b depicting the orientation image maps (OIMs) of structures of the Al sheath and Cu wire (both taken from the peripheral wires' layer radius) of *stacking sequence I*, respectively. The OIMs also depict the low and high angle grain boundaries (LAGBs and HAGBs), featuring the misorientations lower/higher than 15° , as red and black lines, respectively.

The observed grain refinement points to the occurrence of recovery/recrystallization imparted by the severe imposed strain. The grains within the Al components were evidently smaller than within the Cu components, which is primarily given by the fact that the activation energy needed to promote relaxation processes within Al is smaller than the activation energy of Cu [15]. The supposition of occurring recrystallization was confirmed also by the HAGBs analyses (Figs. 3a and 3b show their prevailing portion for both the composite components). The volume fractions of HAGBs, i.e. the boundaries the misorientation angles of which are larger than 15° , were 54% for Cu and 82% for Al within *stacking sequence I*, and 62% for Cu and 79% for Al within *stacking sequence II*. Also, the orientation image mapping showed that the fine grains within all the investigated composite components exhibited no prevailing preferential orientations (i.e. no colour depicting single preferential grains' orientation prevails in the Figures), which confirms the presence of relaxation processes. Fig. 3b also shows that the Cu wires of *stacking sequence I* exhibited the presence of bimodal structure. This phenomenon can be attributed to the effects of the following phenomena: as confirmed above by the observed work hardening and exhaustion of plasticity, the Al sheath of *stacking sequence I* tended to consume the majority of the imposed energy (given by the nature of the RS process and intrinsic properties of Al [15]). Also, the energy needed for grain growth (i.e. secondary recrystallization) is generally up to ten times lower than the energy needed for primary recrystallization [33]. The mutual effect of these phenomena imparted substructure development and grain growth at the expense of further recrystallization during the last swaging pass, which resulted in the formation of bimodal structure within the Cu wires.

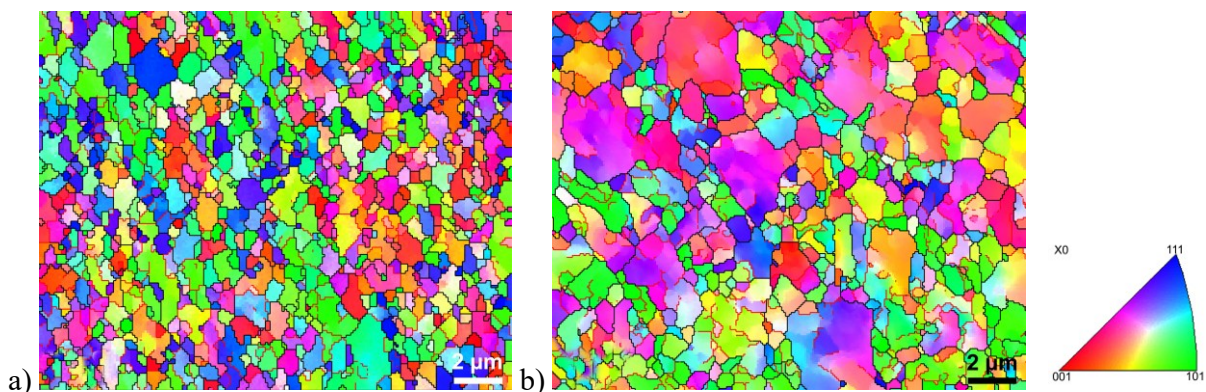


Fig. 3. OIMs with LAGBs depicted in red and HAGBs depicted in black for: Al sheath of *stacking sequence I* (a); Cu wire of *stacking sequence I* (b).

Residual stress. The internal grains misorientations depicting the presence of residual stress within the structures of the Al sheath and Cu wire (both taken from the peripheral wires' layer radius) of *stacking sequence I* are shown in Figs. 4a and 4b, respectively, whereas the internal grains misorientations within the structures of the Cu sheath and Al wire (both taken from the peripheral wires' layer radius) of *stacking sequence II* are shown in Figs. 4c and 4d, respectively.

The results of residual stress analyses showed the grains misorientations, i.e. residual stress, to be locally present in the Cu components of both the stacking sequences. Considering the results of structure analyses, i.e. the presence of bimodal structure within Cu, this phenomenon was primarily caused by the imparted substructure development as the misorientations were mostly observed within the growing grains. The Al components within both the stacking sequences did not exhibit substantial presence of residual stress, which also confirms the suppositions of structure relaxation and occurring recrystallization.

All the structure phenomena are inevitably affected by the two following processing factors. The deformation force affecting the processed material during rotary swaging - consisting of two individual components, radial and axial [2]. The designed composite sequence and the used composite materials – featuring their individual intrinsic properties, such as stacking fault energy, work hardening ability, activation energy for recovery, recrystallization, precipitation, etc. [15]. The plastic flow imparted by the swaging force can non-negligibly affect not only the mechanical properties, but also substructure development and the presence of residual stress within the swaged composites. As documented by the results, the imposed shear strain was sufficient to introduce grain refinement and structure relaxation within the Al components of both the stacking sequences. On the other hand, the Cu components, the activation energy necessary for relaxation processes for which is higher than for Al, exhibited the presence of residual stress. In other words, the occurring recovery/recrystallization was not complete after the last swaging pass for the Cu component, regardless the stacking sequence. Nevertheless, both the final 5 mm composite wires exhibited sufficient bonding of both the components, the present residual stress originating primarily from incomplete substructure development, did not negatively affect any of the composite wires as a whole product.

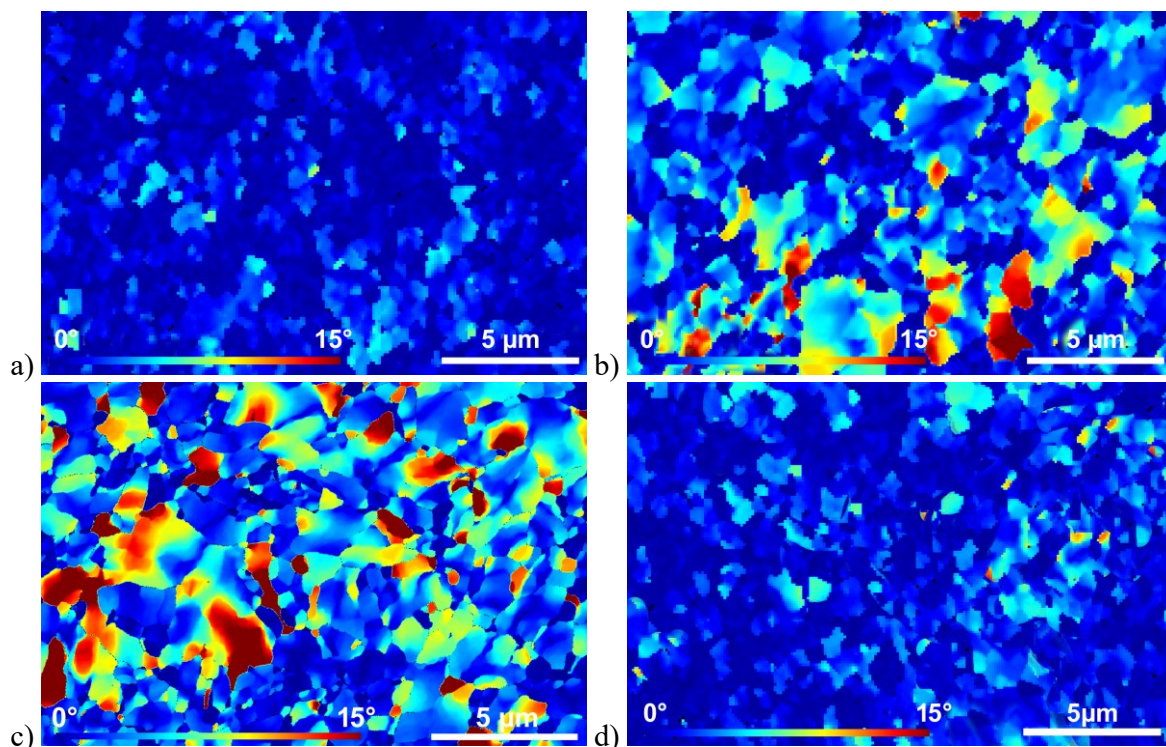


Fig. 4. Grains misorientations pointing to presence of residual stress in rainbow scale from 0° to 15° for: Al sheath of *stacking sequence I* (a); Cu wire of *stacking sequence I* (b); Cu sheath of *stacking sequence II* (c); Al wire of *stacking sequence II* (d).

Conclusions

The presented study proved that the technology of rotary swaging is applicable for production of long electro-conductive Al-Cu clad composite wires; both the swaged composite wires exhibited sufficient bonding of the component metals. The results revealed that, for sufficient swaging ratios, the stacking sequence of the individual metallic components had negligible effects on the substructure development and residual stress within the composite components; both the investigated stacking sequences featured Al components having very fine equiaxed grains with minor presence of residual stress, whereas the Cu components featured bimodal structures with a local presence of residual stress, which was primarily caused by substructure development, i.e. incomplete relaxation during the last swaging pass. Nevertheless, differences between the stacking sequences were observed during mechanical testing. Due to significant work hardening (microhardness over 55 HV) and exhaustion of plasticity of the Al sheath, the composite consisting of Al sheath and Cu wires exhibited very low plasticity (<1%), however, the maximum strength (276 MPa) was comparable to the composite consisting of Cu sheath and Al wires.

References

- [1] S.L. Sing, Characterisation of Titanium-Tantalum Lattice Structures Fabricated by Selective Laser Melting, in: *Sel. Laser Melting Nov. Titanium-Tantalum Alloy as Orthop. Biomater.*, 2019: pp. 87–95. doi:10.1007/978-981-13-2724-7_6.
- [2] R. Kocich, L. Kunčická, D. Dohnalík, A. Macháčková, M. Šofer, Cold rotary swaging of a tungsten heavy alloy: Numerical and experimental investigations, *Int. J. Refract. Met. Hard Mater.* 61 (2016) 264–272. doi:10.1016/j.ijrmhm.2016.10.005.
- [3] T. Hori, T. Nagase, M. Todai, A. Matsugaki, T. Nakano, Development of non-equiatom Ti-Nb-Ta-Zr-Mo high-entropy alloys for metallic biomaterials, *Scr. Mater.* (2019). doi:10.1016/j.scriptamat.2019.07.011.
- [4] X. Huang, J. Miao, A.A. Luo, Lightweight AlCrTiV high-entropy alloys with dual-phase microstructure via microalloying, *J. Mater. Sci.* 54 (2019) 2271–2277. doi:10.1007/s10853-018-2970-4.
- [5] Y. Yan, S. Priya, Multiferroic Magnetolectric Composites/Hybrids, in: C.-S. Kim, C. Randow, T. Sano (Eds.), *Hybrid Hierarchical Compos. Mater.*, Springer International Publishing, Cham, 2015: pp. 95–160. doi:10.1007/978-3-319-12868-9_4.
- [6] Y. Zhao, L. Peng, G. Yu, Electrochemical Hierarchical Composites, in: C.-S. Kim, C. Randow, T. Sano (Eds.), *Hybrid Hierarchical Compos. Mater.*, Springer International Publishing, Cham, 2015: pp. 239–286. doi:10.1007/978-3-319-12868-9_7.
- [7] F. Watari, A. Yokoyama, M. Omori, T. Hirai, H. Kondo, M. Uo, T. Kawasaki, Biocompatibility of materials and development to functionally graded implant for biomedical application, *Compos. Sci. Technol.* 64 (2004) 893–908. doi:10.1016/j.compscitech.2003.09.005.
- [8] S.. Tjong, Z.. Ma, Microstructural and mechanical characteristics of in situ metal matrix composites, *Mater. Sci. Eng. R Reports.* 29 (2000) 49–113. doi:10.1016/S0927-796X(00)00024-3.
- [9] T.W. Clyne, P.J. Withers, *An introduction to metal matrix composites*, New York, NY, USA, 1993.
- [10] L. Kunčická, R. Kocich, K. Dvořák, A. Macháčková, Rotary swaged laminated Cu-Al composites: Effect of structure on residual stress and mechanical and electric properties, *Mater. Sci. Eng. A.* 742 (2019) 743–750. doi:10.1016/j.msea.2018.11.026.
- [11] M. Vaezi, H. Seitz, S. Yang, A review on 3D micro-additive manufacturing technologies, *Int. J. Adv. Manuf. Technol.* 67 (2012) 1721–1754. doi:10.1007/s00170-012-4605-2.

- [12] J. Luo, S. Zhao, C. Zhang, Microstructure of aluminum/copper clad composite fabricated by casting-cold extrusion forming, *J. Cent. South Univ. Technol.* 18 (2011) 1013–1017. doi:10.1007/s11771-011-0796-1.
- [13] R. Kocich, L. Kunčická, C.F. Davis, T.C. Lowe, I. Szurman, A. Macháčková, Deformation behavior of multilayered Al-Cu clad composite during cold-swaging, *Mater. Des.* 90 (2016) 379–388. doi:10.1016/j.matdes.2015.10.145.
- [14] L. Kunčická, R. Kocich, K. Dvořák, A. Macháčková, Rotary swaged laminated Cu-Al composites, Effect of structure on residual stress and mechanical and electric properties, *Mater. Sci. Eng. A.* 742 (2019) 743–750.
- [15] A. Russell, K.L. Lee, *Structure-Property Relations in Nonferrous Metals*, 1st ed., John Wiley & Sons, Inc., New Jersey, 2005.
- [16] A.N. Cherepanov, V.I. Mali, I.N. Maliutina, A.M. Orishich, A.G. Malikov, V.O. Drozdov, Laser welding of stainless steel to titanium using explosively welded composite inserts, *Int. J. Adv. Manuf. Technol.* 90 (2017) 3037–3043. doi:10.1007/s00170-016-9657-2.
- [17] L. Kunčická, R. Kocich, Deformation behaviour of Cu-Al clad composites produced by rotary swaging, *IOP Conf. Ser. Mater. Sci. Eng.* 369 (2018) 012029. doi:10.1088/1757-899X/369/1/012029.
- [18] R. Kocich, M. Kurša, I. Szurman, A. Dlouhý, The influence of imposed strain on the development of microstructure and transformation characteristics of Ni–Ti shape memory alloys, *J. Alloys Compd.* 509 (2011) 2716–2722. doi:10.1016/j.jallcom.2010.12.003.
- [19] M. Suresh, A. Sharma, A.M. More, R. Kalsar, A. Bisht, N. Nayan, S. Suwas, Effect of equal channel angular pressing (ECAP) on the evolution of texture, microstructure and mechanical properties in the Al-Cu-Li alloy AA2195, *J. Alloys Compd.* 785 (2019) 972–983. doi:10.1016/J.JALLCOM.2019.01.161.
- [20] L. Kunčická, R. Kocich, J. Drápala, V.A. Andreyachshenko, FEM simulations and comparison of the ecap and ECAP-PBP influence on Ti6Al4V alloy's deformation behaviour, *Met. 2013 22nd Int. Met. Mater. Conf.* (2013) 391–396.
- [21] R. Kocich, J. Fiala, I. Szurman, A. Macháčková, M. Mihola, Twist-channel angular pressing: effect of the strain path on grain refinement and mechanical properties of copper, *J. Mater. Sci.* 46 (2011) 7865–7876. doi:10.1007/s10853-011-5768-1.
- [22] R. Kocich, L. Kunčická, A. Macháčková, Twist Channel Multi-Angular Pressing (TCMAP) as a method for increasing the efficiency of SPD, *IOP Conf. Ser. Mater. Sci. Eng.* 63 (2014) 012006. doi:10.1088/1757-899X/63/1/012006.
- [23] S.V. Dobatkin, J. Gubicza, D.V. Shangina, N.R. Bochvar, N.Y. Tabachkova, High strength and good electrical conductivity in Cu–Cr alloys processed by severe plastic deformation, *Mater. Lett.* 153 (2015) 5–9. doi:10.1016/J.MATLET.2015.03.144.
- [24] R. Kocich, A. Macháčková, F. Fojtík, Comparison of strain and stress conditions in conventional and ARB rolling processes, *Int. J. Mech. Sci.* 64 (2012) 54–61. doi:10.1016/j.ijmecsci.2012.08.003.
- [25] Y. Yang, J. Nie, Q. Mao, Y. Zhao, Improving the combination of electrical conductivity and tensile strength of Al 1070 by rotary swaging deformation, *Results Phys.* 13 (2019) 102236. doi:10.1016/J.RINP.2019.102236.
- [26] W.M. Gan, Y.D. Huang, R. Wang, G.F. Wang, A. Srinivasan, H.G. Brokmeier, N. Schell, K.U. Kainer, N. Hort, Microstructures and mechanical properties of pure Mg processed by rotary swaging, *Mater. Des.* 63 (2014) 83–88. doi:10.1016/j.matdes.2014.05.057.
- [27] R. Kocich, L. Kunčická, P. Král, P. Strunz, Characterization of innovative rotary swaged Cu-Al clad composite wire conductors, *Mater. Des.* 160 (2018) 828–835. doi:10.1016/j.matdes.2018.10.027.

- [28] L. Kunčická, A. Macháčková, N.P. Lavery, R. Kocich, J.C.T. Cullen, L.M. Hlaváč, Effect of thermomechanical processing via rotary swaging on properties and residual stress within tungsten heavy alloy, *Int. J. Refract. Met. Hard Mater.* 87 (2020) 105120. doi:10.1016/j.ijrmhm.2019.105120.
- [29] L. Kunčická, R. Kocich, C. Hervoche, A. Macháčková, Study of structure and residual stresses in cold rotary swaged tungsten heavy alloy, *Mater. Sci. Eng. A.* 704 (2017) 25–31. doi:10.1016/j.msea.2017.07.096.
- [30] O. Instruments, Providing leading-edge tools for SEM, TEM & FIB - Nanoanalysis -, (2018). <https://nano.oxinst.com/> (accessed December 24, 2018).
- [31] B. Beausir, J.J. Fundenberger, Analysis Tools for Electron and X-ray diffraction, ATEX - software, www.atex-software.eu, (2017).
- [32] R. Kocich, L. Kunčická, A. Macháčková, M. Šofer, Improvement of mechanical and electrical properties of rotary swaged Al-Cu clad composites, *Mater. Des.* 123 (2017) 137–146. doi:10.1016/j.matdes.2017.03.048.
- [33] F.J. Humphreys, M. Hetherly, *Recrystallization and Related Annealing Phenomena*, 2nd ed., Elsevier Ltd, Oxford, 2004.